Rapid Re-Design of Multi-Band Antennas with Respect to Operating Conditions and Material Parameters of Substrate

Slawomir Koziel[1,2], Adrian Bekasiewicz[2]

[1] Engineering Optimization & Modeling Center, Reykjavik University, 101 Reykjavik, Iceland, koziel@ru.is,

[2] Faculty of Electronics, Telecommunications and Informatics, Gdansk University of Technology, 80-233 Gdansk, Poland, bekasiewicz@ru.is

Abstract

This work addresses geometry parameter scaling of multi-band antennas for Internet of Things applications. The presented approach is comprehensive and permits re-design of the structure with respect to both the operating frequencies and material parameters of the dielectric substrate. A two-step procedure is developed with the initial design obtained from an inverse surrogate model constructed using a set of appropriately prepared reference points, and the final design identified through an iterative correction procedure. The latter is necessary in order to account for limited accuracy of the surrogate. The proposed approach is validated using a dual-band microstrip patch antenna scaled over wide ranges of operating frequencies (1.5 GHz to 2.5 GHz for the lower band, and 5.0 GHz to 6.0 GHz for the upper band), substrate thickness (0.7 mm to 1.5 mm), and substrate permittivity (2.5 to 3.5). The re-design cost corresponds to only up to three electromagnetic simulations of the antenna at hand. Reliability of the process is confirmed through experimental validation of the fabricated antenna prototypes.

Keywords: antenna design; multi-band antennas; antenna re-design; surrogate modeling; simulation-driven design.

1. Introduction

The principal challenges of antenna design applications include the necessity of handling multiple performance figures (e.g., matching, gain, efficiency, radiation pattern, size), geometrical complexity (implying a large number of parameters that require tuning), but also utilization of full-wave electromagnetic (EM) analysis for accurate evaluation of radiator performance [16]-[18]. In a typical scenario, antenna is represented using a so-called forward (typically EM-simulation-based) model, which computes response characteristics for a given set of input parameters (i.e., geometric dimensions) [26]. Antenna design using such models involves inverse flow of information oriented towards seeking for a set of unknown adjustable variables for which the structure corresponds to the assumed operating conditions [26]. This process is governed either by parameter sweeps, or numerical optimization algorithms searching for appropriate configuration of variables representing a good match between the achieved and desired performance [1], [2], [8]. The main bottleneck of EM-driven design, especially when the search involves population-based metaheuristics [3]-[6], [19], is the high computational cost [8]. The computational overhead can be reduced, to some extent, using adjoint sensitivities (e.g., [7], [21]), or surrogate-based optimization (SBO) algorithms [8], [9], [22]-[25]. SBO methods applicable to antenna design exploit both data-driven (e.g., kriging [10], co-kriging [22], or neural networks [26]) and EM-based surrogates [8] corrected using appropriate methods (e.g., space mapping [11], manifold mapping [12], or cognition-driven optimization [13]).

Regardless of computational savings resulting from utilization of SBO, or adjoint-based methods, a common problem associated with maintaining low cost of antenna design is to re-design (scale) a particular structure for various operating conditions and/or different dielectric substrates. In practice, due to the necessity of going through the entire process of adjusting all input parameters, utilization of forward models for scaling incurs high

computational cost. Alternatively, re-design can be accelerated using the inverse models. The latter exploit existing designs in order to map the operating conditions of the antenna onto configurations of parameters corresponding to designs that are optimum w.r.t. to these conditions [14], [27]. For structures with simple topologies, represented using either analytical or equivalent circuit models [29], the dimensions can be extracted using design curves [28], [29]. Design curves illustrate variability of input parameters as a function of the selected performance figure, which is convenient for tracking their changes (typically, using a visual inspection) within the range of the assumed operating conditions [29]. On the other hand, they are unsuitable for handling multiple performance figures, or complex mutual interactions between the parameters [30], [31]. A more generic approach involves antenna re-design using approximation-based models, which are useful for solving problems characterized by multiple operating conditions [15].

Inverse models can be constructed from a set of pre-defined reference designs. The cost of identifying the reference designs can be reduced by replacing high-fidelity EM forward models with their coarsely-discretized counterparts which are 10- to 50-fold faster, but also less accurate [8], [14]. The loss of accuracy can be compensated using appropriate correction techniques [8], [14], [15]. Once the inverse model is identified, it can be re-used multiple times at a negligible cost. A technique for dimension scaling of narrow-band antennas with respect to the operating frequency that exploits approximation-based inverse models has been proposed in [14]. In [15], the method has been applied to dual-band antennas.

Antenna performance depends on its dimensions, but also the electrical/mechanical properties of materials it is implemented on. In case of planar radiators, modification of the substrate parameters—dictated either by manufacturing-related constraints or specific application setup—drastically affects the response characteristics. For multi-band structures,

the problem becomes even more challenging due to complex interactions between the antenna parameters and substrate properties and antenna characteristics. In this work, the concept of inverse surrogate modeling is extended to dimension scaling of dual-band antennas with respect to operating frequencies and parameters of the dielectric substrate material (i.e., permittivity and thickness). In our numerical experiments, four figures of interest are handled simultaneously which makes the re-design process significantly more challenging than in [15], because limited reliability of the inverse surrogate leads to accumulation of the scaling errors. Here, an iterative procedure has been proposed that allows for precise allocation of the operating frequencies at the cost of up to three EM simulations of the antenna at hand. Our approach is demonstrated using a dual-band quasi-patch antenna scaled with respect to both operating frequencies that cover industrial, scientific, and medical radio bands (1.5 GHz to 2.5 GHz, and 5.0 GHz to 6.0 GHz, for lower and upper band, respectively) and substrate parameters (0.7 mm to 1.5 mm for the thickness, and 2.5 to 3.5 for permittivity). Comprehensive verification study (both numerical and experimental) confirms reliability of the proposed technique.

2. Antenna Scaling for Operating Conditions and Material Parameters

The purpose of this section is to formulate the dimension scaling task for antennas and describe the basic components of the scaling procedure, including the introduced inverse surrogate model that accounts for performance figures and material parameters, as well as the proposed scheme for iterative correction of the model errors.

2.1. Dimension Scaling of Multi-Band Antennas

The primary (high-fidelity) EM-simulation model of the antenna structure under design will be denoted as $\boldsymbol{R}_f(\boldsymbol{x})$ with $\boldsymbol{x} = [x_1 \ \ldots \ x_n]^T$ being a vector of geometry parameters. We also denote by h (thickness) and ε_r (permittivity) the substrate parameters. Given the

operating frequencies $f_{0.1}$, $f_{0.2}$, through $f_{0.p}$ (p is the number of antenna bands) and the substrate parameters h_0, ε_{r0}, $\boldsymbol{x}_f^*(f_{0.1},f_{0.2},\ldots,f_{0.p};h_0,\varepsilon_{r0})$ will denote the corresponding set of optimum antenna dimensions (i.e., optimized parameters that allocate the operating frequencies as required for antenna implemented on the substrate of thickness h_0 and permittivity ε_r). The scaling problem is formulated as follows: given $\boldsymbol{x}_f^*(f_{0.1},\ldots,f_{0.p};h_0,\varepsilon_{r0})$, find $\boldsymbol{x}_f^*(f_1,\ldots,f_p;h,\varepsilon_r)$, i.e., optimum parameter values of the antenna implemented on the substrate of thickness h and dielectric permittivity ε_r, and having its operating frequencies allocated at f_1, f_2, through f_p. The re-design process should be enabled for the user-defined ranges, $f_{k\min} \le f_k \le f_{k\max}$, $k = 1, \ldots, p$, $h_{\min} \le h \le h_{\max}$, and $\varepsilon_{r\min} \le \varepsilon_r \le \varepsilon_{r\max}$.

2.2. Reference Designs and Inverse Surrogate Model

Let $\{f_{1.j},f_{2.j},\ldots,f_{p.j},h_j,\varepsilon_{r.j}\}$, $j = 1, \ldots, N_r$, be a preselected set of operating conditions, allocated within the ranges defined in Section 2.1. The antenna is optimized at the level of coarse-discretization EM model $\boldsymbol{R}_c$ to find $\boldsymbol{x}_c^*(f_{1.j},\ldots,f_{p.j};h_j,\varepsilon_{r.j})$, referred to as reference designs.

In the next step, an inverse surrogate model $\boldsymbol{x}_c(f_1,\ldots,f_p;h,\varepsilon_r)$ is defined as

$$\boldsymbol{x}_c(f_1,\ldots,f_p;h,\varepsilon_r;\boldsymbol{P}) = \left[x_{c.1}(f_1,\ldots,f_p;h,\varepsilon_r;\boldsymbol{p}_1)\ \ldots\ x_{c.n}(f_1,\ldots,f_p;h,\varepsilon_r;\boldsymbol{p}_n)\right]^T \tag{1}$$

in which $x_{c.l}(f_1,\ldots,f_p;h,\varepsilon_r,\boldsymbol{p}_l)$ is a model of the lth geometry parameter. $\boldsymbol{P} = [\boldsymbol{p}_1\ \ldots\ \boldsymbol{p}_n]$ is the overall parameter vector.

The choice of an appropriate analytical form of the surrogate is of importance. The model should be sufficiently flexible to account for dependence between geometry parameters and operating frequencies but, at the same time, the number of parameters should be limited to avoid modeling local fluctuations (e.g., being a result of inaccurate optimization of particular reference designs). Here, we set

$$x_{c.l}(f_1,...,f_p;h,\varepsilon_r)=\left[\prod_{l=1}^{p}s_{f.l}(f_l)\right]s_{h.l}(h)s_{\varepsilon_r.l}(\varepsilon_r)q_l(f_0,K,h,\varepsilon_r) \tag{2}$$

where the individual parameter dependencies are modeled using exponential functions

$$\begin{gathered}s_{f.l}(f_l)=a_{f.l.1}+a_{f.l.2}\exp(a_{f.l.3}f_l),\quad l=1,...,p\\ s_{h.l}(h)=a_{h.1}+a_{h.2}\exp(a_{h.3}h)\\ s_{\varepsilon_r.l}(\varepsilon_r)=a_{\varepsilon_r.1}+a_{\varepsilon_r.2}\exp(a_{\varepsilon_r.3}\varepsilon_r)\end{gathered} \tag{3}$$

The reason for using exponential functions in (3) is that they are well suited to account for the typical relationships between antenna dimensions and the operating frequencies and substrate parameters, including the saturation effects (often observed for lateral parameters), and provide sufficient flexibility. Also, small number of coefficients facilitates identification of the surrogate using a limited number of reference designs. Parameter interdependence is accounted for by a second-order term

$$\begin{gathered}q_l(f_1,...,f_p,h,\varepsilon_r)=a_{q.0}+a_{q.1}f_1+...+a_{q.p}f_p+a_{q.p+1}h+a_{q.p+2}\varepsilon_r+\\ a_{q.p+3}f_1^2+...+a_{q.2p+2}f_p^2+a_{q.2p+3}h^2+a_{q.2p+4}\varepsilon_r^2+\\ +a_{q.2p+5}f_1f_2+\ ...\ +a_{q.(p^2+7p+12)/2}h\varepsilon_r\end{gathered} \tag{4}$$

The total number of parameters of q_l is $(p^2 + 7p + 12)/2$. The model parameters are found using Matlab's *lsqnonlin* curve fitting function as

$$\boldsymbol{p}_l=\arg\min_{\boldsymbol{p}}\sum_{j=1}^{N_r}(x_{c.l}(f_{1.j},...,f_{2.j};h_j,\varepsilon_{r.j},\boldsymbol{p})-x_{c.j.l})^2 \tag{5}$$

where $\boldsymbol{x}_{c.j} = [x_{c.j.1}\ \ \ldots\ \ x_{c.j.n}]^T$ is the reference design corresponding to the operating frequencies $f_{1.j}, \ldots, f_{p.j}$, and the substrate parameters h_j and $\varepsilon_{r.j}$.

In order to ensure uniqueness of model identification, the number of reference designs has to be larger or equal than the number of model parameters. On the other hand, to smoothen out local fluctuations mentioned above, N_r should be considerably larger. The specific data concerning a verification example considered in this work is given in Section 3.

2.3. Scaling Procedure

The re-designed antenna dimensions are found by evaluating the following expression:

$$\boldsymbol{x}_f(f_1,\ldots,f_p;h,\varepsilon_r)=\boldsymbol{x}_c(f_1,\ldots,f_p;h,\varepsilon_r,\boldsymbol{P})+\left[\boldsymbol{x}_f^*(f_{0.1},\ldots,f_{0.p};h_0,\varepsilon_{r.0})-\boldsymbol{x}_c^*(f_{0.1},\ldots,f_{0.p};h_0,\varepsilon_{r.0})\right] \quad (6)$$

The term $\boldsymbol{x}_f^*(f_{0.1}, f_{0.2}, \ldots, f_{0.p}; h_0, \varepsilon_{r0}) - \boldsymbol{x}_c^*(f_{0.1}, f_{0.2}, \ldots, f_{0.p}; h_0, \varepsilon_{r0})$ is introduced in order to align $\boldsymbol{x}_c(.)$ with the high-fidelity model at the operating conditions of $\{f_{0.1}, f_{0.2}, \ldots, f_{0.p}, h_0, \varepsilon_{r0}\}$. This is necessary because the surrogate (1) has been constructed at the level of coarse-discretization model $\boldsymbol{R}_c$.

2.4. Iterative Design Correction

The formula (6) delivers ideal scaling under the assumption of perfect correlation between the low- and high-fidelity EM models as well as error-less representation of the reference designs by the surrogate. Neither is the case in practice, therefore, scaling errors are expected. We denote by Δf_k the differences between the required and the actual operating frequencies. The following procedure is utilized to correct these errors:

$$\begin{aligned}\boldsymbol{x}_f(f_1,\ldots,f_p;h,\varepsilon_r) \leftarrow \boldsymbol{x}_c(f_1-\textstyle\sum_{k=1}^{i}\Delta f_{1.k},\ldots,f_p-\sum_{k=1}^{i}\Delta f_{p.k};h,\varepsilon_r,\boldsymbol{P})+\\ +\left[\boldsymbol{x}_f^*(f_{0.1},\ldots,f_{0.p};h_0,\varepsilon_{r.0})-\boldsymbol{x}_c^*(f_{0.1},\ldots,f_{0.p};h_0,\varepsilon_{r.0})\right]\end{aligned} \quad (7)$$

The procedure incorporates the scaling errors accumulated over the iterations of (7) into subsequent evaluation of the surrogate model. From our experience, two or three iterations are sufficient for the procedure to converge. Expense-wise, each iteration requires only one high-fidelity EM simulation of the antenna so that the overall re-design cost is low.

3. Verification Cases

Consider a dual-band planar antenna shown in Fig. 1 [15]. The structure consists of two radiating elements in the form of a quasi-microstrip patch with inset feed and a monopole radiator. The adjustable parameters $\boldsymbol{x} = [L\ l_1\ l_2\ l_3\ W\ w_1\ w_2\ g]^T$ are selected based on analysis of

antenna sensitivity [8]. Dimensions o = 7, l_0 = 10 and s = 0.5 are fixed (all dimensions in mm); w_0 is calculated for a given substrate permittivity and thickness to ensure 50 ohm input impedance. The EM models of the antenna are implemented in CST Microwave Studio [20]: high-fidelity $\boldsymbol{R}_f$ (~1,200,000 hexahedral mesh cells, simulation time: 6 min), and low-fidelity $\boldsymbol{R}_c$ (~130,000 cells, simulation: 35 s). The EM simulations are performed using time domain solver [20].

The objective is to re-design the antenna with respect to four figures of interest including operating frequencies within ranges of 1.5 GHz $\leq f_1 \leq$ 2.5 GHz and 5.0 GHz $\leq f_2 \leq$ 6.0 GHz, as well as substrate thickness and permittivity between 0.7 mm $\leq h \leq$ 1.5 mm and 2.5 $\leq \varepsilon_r \leq$ 3.5, respectively. As reference designs we consider all the combinations (a total of 81) of $f_1 \in \{1.5, 2.0, 2.5\}$, $f_2 \in \{5.0, 5.5, 6.0\}$, $h \in \{0.7, 1.1, 1.5\}$, and $\varepsilon_r \in \{2.5, 3.0, 3.5\}$. The high-fidelity reference design obtained at the domain center is $\boldsymbol{x}_f^*(2.0,5.5;1.1,3.0)$ = [15.9 5.22 13.0 5.88 16.6 0.25 9.03 6.83]^T, whereas its corresponding low-fidelity design is $\boldsymbol{x}_c^*(2.0,5.5;1.1,3.0)$ = [15.8 5.25 12.9 5.86 16.7 0.2 9.05 6.81]^T.

The inverse surrogate model is constructed as described in Section 2.2. Its selected two-dimensional cuts are shown in Fig. 2. It can be observed that while the surrogate properly reflects the main trends (as relationships between the operating conditions and geometry parameters), certain errors are noticeable (i.e., the model only provides an approximation of the training samples). This is why the iterative correction procedure (7) is essential for the reliability of the scaling process.

A comprehensive verification of the procedure has been conducted. Table 1 gathers the twelve sets of operating frequencies and substrate parameters (corresponding to practically used bands and popular substrate laminates) for which the considered antenna structure has been re-designed. As indicated in the last two columns of Table 1, the allocation of the operating frequencies is nearly perfect. Fig. 3 shows the EM-simulated reflection responses

obtained for six selected designs. The total scaling cost in all cases is three evaluations of the high-fidelity model. Five selected designs have been fabricated and measured. These are $\boldsymbol{x}^{(2)}$ = [13.9 7.53 15 2 4.79 18.4 0.69 11.0 9.2]^T, $\boldsymbol{x}^{(5)}$ = [16.3 7.38 15.5 5.74 18.8 0.83 11.2 9.8]^T, $\boldsymbol{x}^{(8)}$ = [14.1 6.29 14.7 4.7 18.1 1.53 10.2 8.2]^T, $\boldsymbol{x}^{(10)}$ = [16.0 5.8 14.2 5.1 18.0 2.8 9.85 7.87]^T, and $\boldsymbol{x}^{(11)}$ = [16.8 5.68 14.6 5.57 18.3 2.39 9.8 8.95]^T. Designs $\boldsymbol{x}^{(2)}$, $\boldsymbol{x}^{(8)}$ and $\boldsymbol{x}^{(10)}$ are implemented on a Rogers RO4003C substrate, whereas $\boldsymbol{x}^{(5)}$ and $\boldsymbol{x}^{(11)}$ on an AD250C laminate.

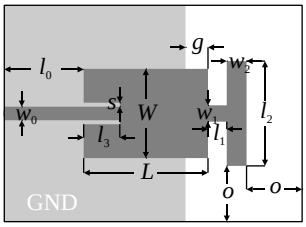

Fig. 1. Geometry of the dual-band patch antenna [15].

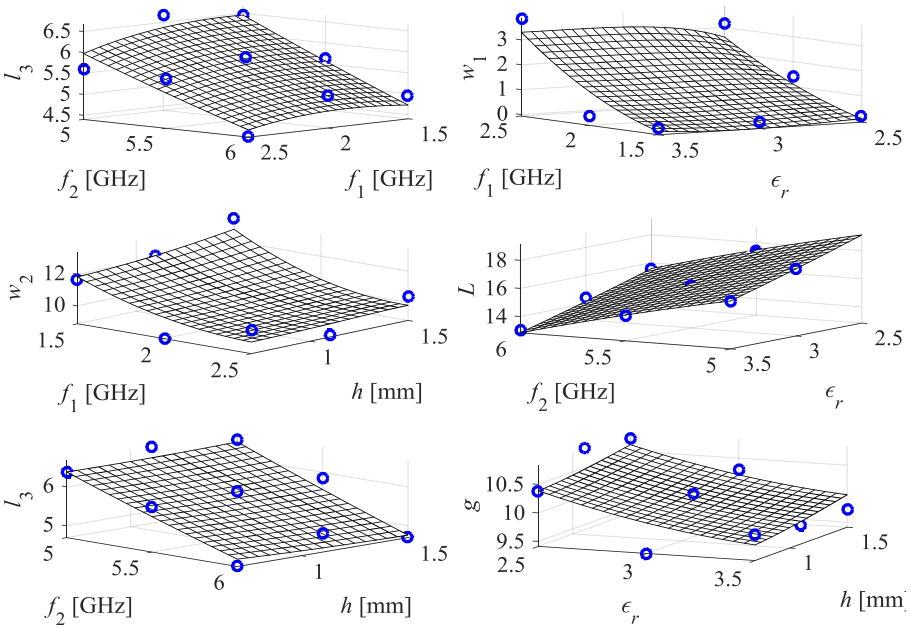

Fig. 2. Dual-band antenna structure: selected two-dimensional projections of the inverse surrogate model mapping four inputs (i.e., figures of interest) to antenna geometry parameters (only selected dimensions are visualized). Remaining operating conditions and substrate parameters are set at the domain center (i.e., f_1 = 2.0 GHz, f_2 = 5.5 GHz, h = 1.1 mm, ε_r = 3.0).

Table 1. Verification Cases for Dual-Band Antenna

No.	Verification case				Obtained operating conditions	
	Operating conditions		Substrate parameters			
	f_1 [GHz]	f_2 [GHz]	h [mm]	ε_r	f_1 [GHz]	f_2 [GHz]
1	1.75	5.30	1.524	3.38	1.75	5.30
2	1.75	5.775	0.813	3.38	1.76	5.776
3	1.75	5.65	1.524	2.97	1.75	5.65
4	1.845	5.30	1.524	3.38	1.85	5.30

5	1.845	5.775	0.762	2.50	1.85	5.770
6	1.845	5.65	0.813	3.38	1.85	5.65
7	2.15	5.30	1.524	2.97	2.15	5.30
8	2.15	5.775	1.524	3.38	2.15	5.776
9	2.15	5.65	0.813	3.38	2.16	5.65
10	2.45	5.30	1.524	3.38	2.45	5.30
11	2.45	5.775	0.762	2.50	2.47	5.775
12	2.45	5.65	1.524	2.97	2.45	5.65

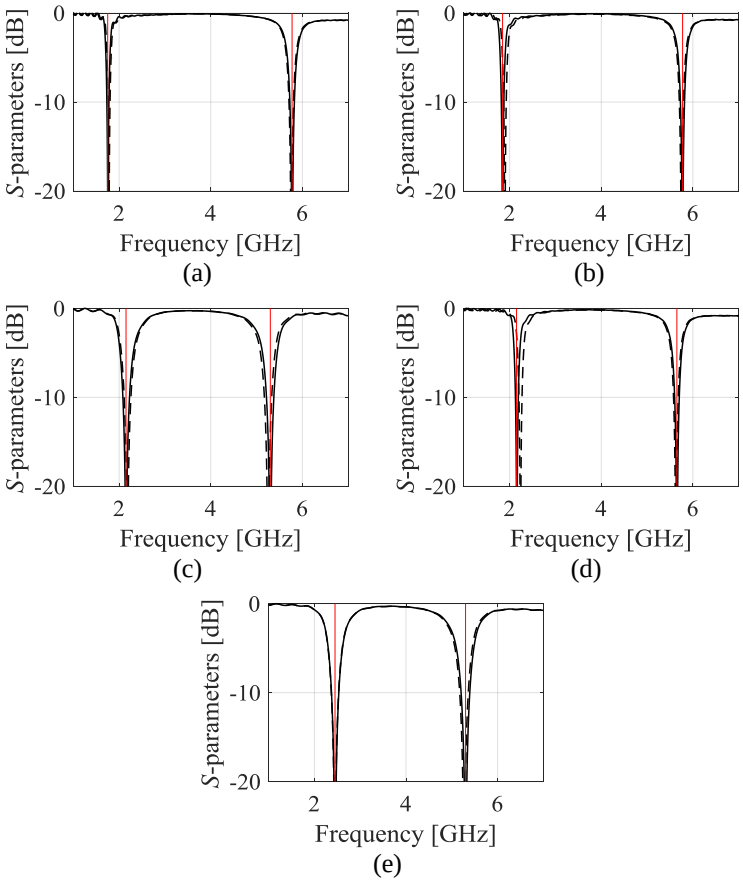

Fig. 3. Verification cases: patch antenna response before iterative correction (– –) and the final design (—). Required operating frequencies have been marked using vertical lines. Antenna structure scaled for: (**a**) [f_1 f_2 h ε_r] = [1.75 5.775 0.813 3.38], (**b**) [f_1 f_2 h ε_r] = [1.845 5.775 2.50 0.762], (**c**) [f_1 f_2 h ε_r] = [2.15 5.30 2.97 1.524], (**d**) [f_1 f_2 h ε_r] = [2.15 5.65 3.38 0.813], and (**e**) [f_1 f_2 h ε_r] = [2.45 5.30 3.38 1.524].

Figure 4 shows the photographs of the fabricated antennas, whereas Figs. 5 to 7 show the reflection responses, H-plane, and E-plane patterns at the operating frequencies, respectively. The operational bandwidth of the antenna is between 2% to around 5% which is typical for the considered structure. The agreement between simulations and measurements is very good. The slight shifts for reflection characteristics are mostly because the SMA connectors were

not included in the EM models, whereas discrepancies for E-plane patterns result from the shadowing effect of the measurement setup (90-degree bend used to mount the antenna).

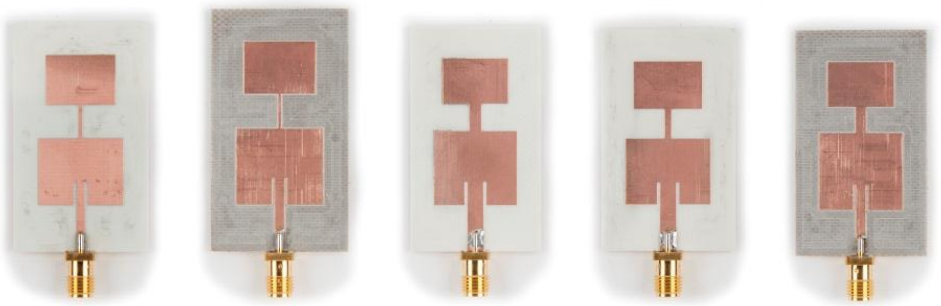

(a) (b) (c) (d) (e)

Fig. 4. Photographs of the manufactured antenna prototypes: (a) $\boldsymbol{x}^{(2)}$, (b) $\boldsymbol{x}^{(5)}$, (c) $\boldsymbol{x}^{(8)}$, (d) $\boldsymbol{x}^{(10)}$, and (e) $\boldsymbol{x}^{(11)}$.

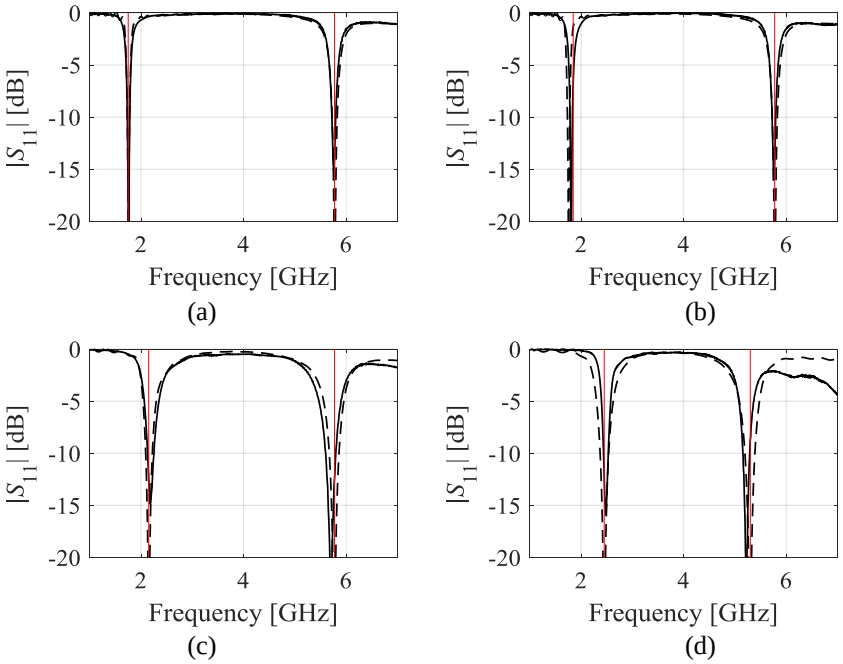

Fig. 5. Comparison of simulated (– –) and measured (—) reflection characteristics obtained for selected antenna designs: (a) $\boldsymbol{x}^{(2)}$, (b) $\boldsymbol{x}^{(5)}$, (c) $\boldsymbol{x}^{(8)}$, and (d) $\boldsymbol{x}^{(10)}$.

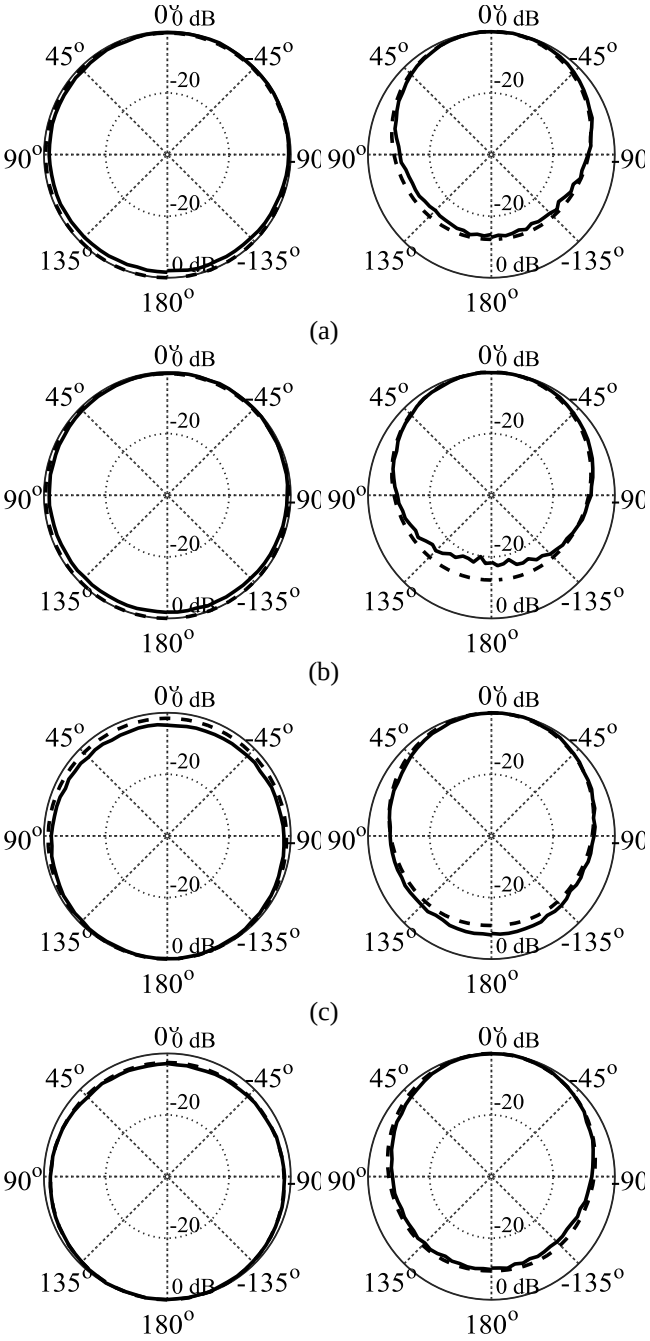

Fig. 6. Comparison of simulated (– –) and measured (—) H-plane radiation patterns obtained for the selected antenna designs: (a) $\boldsymbol{x}^{(2)}$, (b) $\boldsymbol{x}^{(5)}$, (c) $\boldsymbol{x}^{(8)}$, and (d) $\boldsymbol{x}^{(10)}$.

4. Conclusion

A technique for computationally efficient multi-band antenna re-design, simultaneously with respect to operating conditions and parameters of the substrate material has been presented. Our approach involves utilization of an inverse surrogate model constructed from a set of coarsely-discretized reference designs. The accuracy of the scaling

process is ensured by an iterative correction procedure which accounts for accumulated errors of the model. Comprehensive validation, both numerical and experimental demonstrates reliability of the method, as well as a wide scaling range. The proposed technique is useful for rapid re-design of antenna structures represented using expensive EM-simulation models.

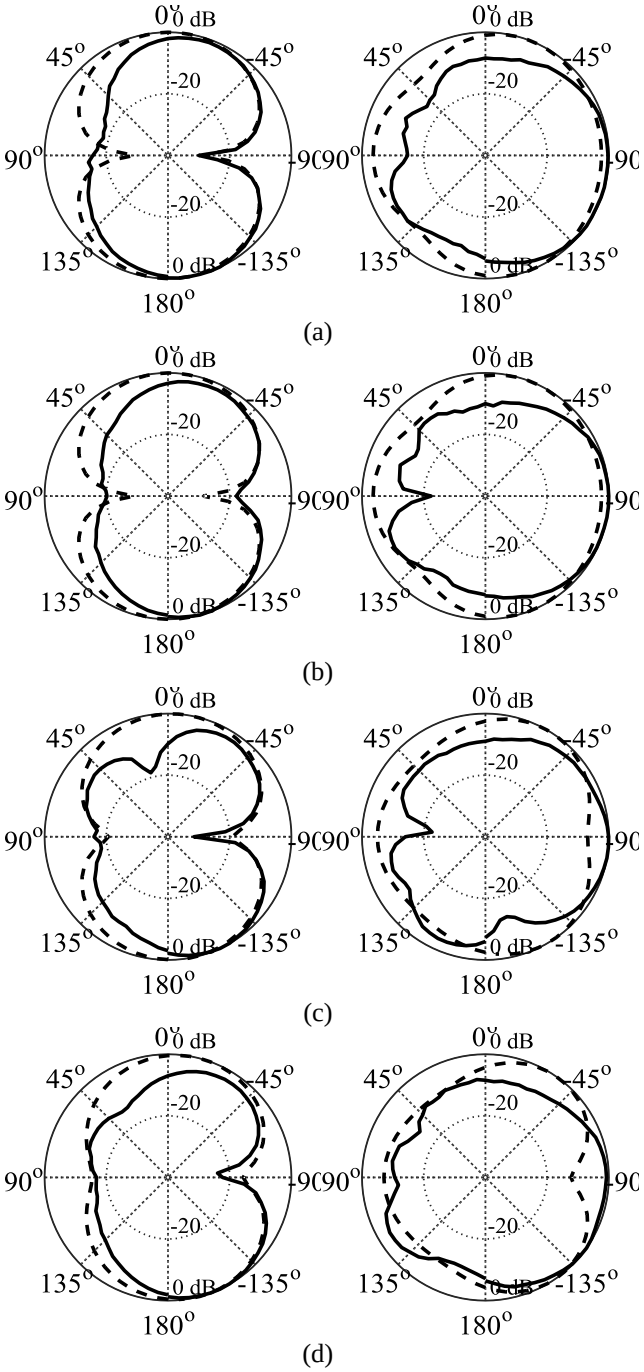

Fig. 7. Comparison of simulated (– –) and measured (—) E-plane patterns obtained for the selected antenna designs: (a) $\boldsymbol{x}^{(2)}$, (b) $\boldsymbol{x}^{(5)}$, (c) $\boldsymbol{x}^{(8)}$, (d) $\boldsymbol{x}^{(10)}$.

Fast dimension scaling is of paramount importance for lowering the cost of adjusting the antenna properties for various application scenarios determined not only by the operating frequencies, but also the properties of the utilized substrate materials. Future work will focus on adaptation of the approach to other microwave components.

Acknowledgment

The authors would like to thank Dassault Systemes, France, for making CST Microwave Studio available. This work was supported in part by the Icelandic Centre for Research (RANNIS) Grant 174114051, and by National Science Centre of Poland Grant 2018/31/B/ST7/02369.

References

[1] J. Nocedal and S. Wright, *Numerical Optimization,* 2nd edition, Springer, New York, 2006.

[2] D.B. Rodrigues, P.F. Maccarini, S. Salahi, T.R. Oliveira, P.J.S. Pereira, P. Limao-Vieira, B.W. Snow, D. Reudink, and P.R. Stauffer, "Design and optimization of an ultra wideband and compact microwave antenna for radiometric monitoring of brain temperature," *IEEE Trans. Biomedical Eng.*, vol. 61, no. 7, pp. 2154-2160, 2014.

[3] Y.H. Chiu and Y.S. Chen, "Multi-objective optimization of UWB antennas in impedance matching, gain, and fidelity factor," *Int. Symp. Ant. Prop.*, pp. 1940-1941, 2015.

[4] Y.S. Chen, "Frequency-domain and time-domain performance enhancements of ultra-wideband antennas using multiobjective optimization techniques," *European Ant. Prop. Conf.*, pp. 1-4, 2016.

[5] S. K. Goudos, K. Siakavara, T. Samaras, E. E. Vafiadis, and J. N. Sahalos, "Self-adaptive differential evolution applied to real-valued antenna and microwave design problems," *IEEE Trans. Antennas Propag.*, vol. 59, no. 4, pp. 1286–1298, Apr. 2011.

[6] A.A. Al-Azza, A.A. Al-Jodah, and F.J. Harackiewicz, "Spide monkey optimization: a novel technique for antenna optimization," *IEEE Ant. Wireless Prop. Lett.*, vol. 15, pp. 1016-1019, 2016.

[7] M.A. El Sabbagh, M.H. Bakr, and J.W. Bandler, "Adjoint higher order sensitivities for fast full-wave optimization of microwave filters," *IEEE Trans. Microw Theory Tech.*, vol. 54, pp. 3339-3351, 2006.

[8] S. Koziel and S. Ogurtsov, "Antenna design by simulation-driven optimization. Surrogate-based approach," Springer, 2014.

[9] J.A. Easum, J. Nagar, and D.H. Werner, "Multi-objective surrogate-assisted optimization applied to patch antenna design," *Int. Symp. Ant. Prop.*, pp. 339-340, San Diego, 2017.

[10] D.I.L. de Villiers, I. Couckuyt, and T. Dhaene, "Multi-objective optimization of reflector antennas using kriging and probability of improvement," *Int. Symp. Ant. Prop.*, pp. 985-986, San Diego, 2017.

[11] J.W. Bandler, Q.S. Cheng, S.A. Dakroury, A.S. Mohamed, M.H. Bakr, K. Madsen, and J. Søndergaard, "Space mapping: the state of the art," *IEEE Trans. Microwave Theory Tech.*, vol. 52, no. 1, pp. 337-361, 2004.

[12] D. Echeverría Ciaurri and P. Hemker, "Manifold mapping: A two-level optimization technique," *Computing and Visualization in Science*, vol. 11, pp. 193-206, 2006.

[13] C. Zhang, F. Feng, V. Gongal-Reddy, Q.J. Zhang, and J.W. Bandler, "Cognition-Driven Formulation of Space Mapping for Equal-Ripple Optimization of Microwave Filters," IEEE Trans. Microwave Theory Tech., vol. 63, no. 7, pp. 2154-2165, 2015.

[14] S. Koziel, and A. Bekasiewicz, "Inverse surrogate modeling for low-cost geometry scaling of microwave and antenna structures," *Eng. Comp.*, vol. 33, no. 4, pp. 1095-1116, 2016.

[15] S. Koziel and A. Bekasiewicz, "Rapid dimension scaling of dual-band antennas using variable-fidelity EM models and inverse surrogates," *J. EM Waves and Applications*, vol.31, no. 3, pp. 297-308, 2017.

[16] K.R. Jha, B. Bukhari, C. Singh, G. Mishra and S. K. Sharma, "Compact planar multistandard MIMO antenna for IoT applications," *IEEE Trans. Ant. Prop.*, vol. 66, no. 7, pp. 3327-3336, 2018.

[17] Rahman, M.; Park, J.-D. The Smallest Form Factor UWB Antenna with Quintuple Rejection Bands for IoT Applications Utilizing RSRR and RCSRR. *Sensors* 2018, *18*, 911.

[18] Rahman, M.; NaghshvarianJahromi, M.; Mirjavadi, S.S.; Hamouda, A.M. Resonator Based Switching Technique between Ultra Wide Band (UWB) and Single/Dual Continuously Tunable-Notch Behaviors in UWB Radar for Wireless Vital Signs Monitoring. *Sensors* 2018, *18*, 3330.

[19] Januszkiewicz, Ł.; Di Barba, P.; Jopek, Ł.; Hausman, S. Many-Objective Automated Optimization of a Four-Band Antenna for Multiband Wireless Sensor Networks. *Sensors* 2018, *18*, 3309.

[20] CST Microwave Studio, ver. 2013, Dassault Systems, 10 rue Marcel Dassault, CS 40501, Vélizy-Villacoublay Cedex, France, 2013.

[21] M.H. Bakr and N.K. Nikolova, "An adjoint variable method for time-domain transmission-line modeling with fixed structured grids," *IEEE Trans. Microwave Theory Tech.*, vol. 52, no. 2, pp. 554-559, 2004.

[22] A.I.J. Forrester, and A.J. Keane, "Recent advances in surrogate-based optimization," *Prog. Aerospace Sci.*, vol. 45, pp. 50-79, 2009.

[23] N.V. Queipo, R.T. Haftka, W. Shyy, T. Goel, R. Vaidynathan, and P.K. Tucker, "Surrogate-based analysis and optimization," *Prog. Aerospace Sci.*, vol. 41, no. 1, pp. 1-28, Jan. 2005.

[24] F. Feng, C. Zhang, W. Na, J. Zhang, W. Zhang, and Q. Zhang, "Adaptive feature zero assisted surrogate-based EM optimization for microwave filter design," *IEEE Microwave Wireless Comp. Lett.*, vol. 29, no. 1, pp. 2-4, 2019.

[25] F. E. Rangel-Patiño, J. L. Chávez-Hurtado, A. Viveros-Wacher, J. E. Rayas-Sánchez and N. Hakim, "System margining surrogate-based optimization in post-silicon validation," *IEEE Trans. Microwave Theory Techn.*, vol. 65, no. 9, pp. 3109-3115, 2017.

[26] H. Kabir, Y. Wang, M. Yu, and Q.J. Zhang, "Neural network inverse modeling and applications to microwave filter design," *IEEE Trans. Microwave Theory Tech.*, vol. 56, no. 4, pp. 867-879, 2008.

[27] G. Gosal, E. Almajali, D. McNamara, and M. Yagoub, "Transmitarray antenna design using forward and inverse neural network modeling," *IEEE Ant. Wireless Prop. Lett.*, vol. 15, pp. 1483-1486, 2016.

[28] M. Caenepeel, F. Ferranti, and Y. Rolain, "Efficient and automated generation of multidimensional design curves for coupled-resonator filters using system identification and metamodels," *Int. Conf. Synthesis, Modeling, Analysis Sim. Methods App. Circuit Design*, Lisbon, 2016.

[29] P.S. Kildal, E. Olsen, and J.A. Aas, "Losses, sidelobes, and cross polarization caused by feed-support struts in reflector antennas: design curves," *IEEE Trans. Ant. Prop.*, vol. 36, no. 2, pp. 182-190, 1988.

[30] A. Mukhopadhay, S. Bhattacharya, R. Roy, S. Fodder and S. Sengupta, "Design of microstrip patch antenna enriched with curve-fitting approach," *Industrial Automation Electromechanical Eng. Conf.*, Bangkok, pp. 214-216, 2017.

[31] M. Narducci, E. Figueras, I. Gracia, L. Fonseca, J. Santander, and C. Cane, "Dimension-scaling of microcantilevers resonators," *Spanish Conf. Electron Devol.*, Madrid, pp. 209-211, 2007.